Published online 18 July 2016

Nucleic Acids Research, 2016, Vol. 44, No. 20 ***9667–9680***
doi: 10.1093/nar/gkw643

Tunable regulation of CREB DNA binding activity couples genotoxic stress response and metabolism

Sang Hwa Kim[1], Anthony T. Trinh[1], Michele Campaigne Larsen[2], Adam S. Mastrocola[1], Colin R. Jefcoate[2], Pierre R. Bushel[3] and Randal S. Tibbetts[1,*]

[1]Department of Human Oncology, University of Wisconsin-Madison School of Medicine and Public Health, Madison, WI 53705, USA, [2]Department of Cell and Regenerative Biology, University of Wisconsin-Madison School of Medicine and Public Health, Madison, WI 53705, USA and [3]Biostatistics and Computational Biology Branch, National Institute of Environmental Health Sciences, Research Triangle Park, NC 27709, USA

Received May 31, 2016; Revised July 6, 2016; Accepted July 8, 2016

ABSTRACT

cAMP response element binding protein (CREB) is a key regulator of glucose metabolism and synaptic plasticity that is canonically regulated through recruitment of transcriptional coactivators. Here we show that phosphorylation of CREB on a conserved cluster of Ser residues (the ATM/CK cluster) by the DNA damage-activated protein kinase ataxia-telangiectasia-mutated (ATM) and casein kinase1 (CK1) and casein kinase2 (CK2) positively and negatively regulates CREB-mediated transcription in a signal dependent manner. In response to genotoxic stress, phosphorylation of the ATM/CK cluster inhibited CREB-mediated gene expression, DNA binding activity and chromatin occupancy proportional to the number of modified Ser residues. Paradoxically, substoichiometric, ATM-independent, phosphorylation of the ATM/CK cluster potentiated bursts in CREB-mediated transcription by promoting recruitment of the CREB coactivator, cAMP-regulated transcriptional coactivators (CRTC2). Livers from mice expressing a non-phosphorylatable CREB allele failed to attenuate gluconeogenic genes in response to DNA damage or fully activate the same genes in response to glucagon. We propose that phosphorylation-dependent regulation of DNA binding activity evolved as a tunable mechanism to control CREB transcriptional output and promote metabolic homeostasis in response to rapidly changing environmental conditions.

INTRODUCTION

cAMP response element binding protein (CREB) is a ubiquitously expressed bZIP family transcription factor (TF) that has served as a paradigm for stimulus-induced transcription for more than 25 years (1). CREB and the closely related proteins Activating Transcription Factor 1 (ATF1) and cAMP response element modulator (CREM), comprise a subfamily of bZIP TFs that share high homology in their intrinsically disordered KID and bZIP DNA-binding domains. CREB binds to palindromic (TGACGTCA) or half-site (TGAC/G) cyclic AMP response elements (CREs) that typically occur within several kb of a transcription start site. Chromatin immunoprecipitation (ChIP) and *in silico*-based strategies suggest that CREB occupies several thousand genes; though only a fraction of these genes are responsive to CREB-activating stimuli (2,3). Physiologic roles of CREB are best understood in the contexts of metabolic regulation—where CREB promotes hepatic gluconeogenesis (1,4)—and memory formation, where CREB contributes to long-term potentiation in organisms as diverse as Aplysia and mice (2,3,5).

The canonical CREB activation pathway involves its phosphorylation on S133 by protein kinase A (PKA) (6–9), which causes the unstructured KID to fold into orthogonal helices that associate with the KID-interacting (KIX) domain of CREB-binding protein (CBP) (10,11). Recruitment of CBP to CREB-loaded promoters triggers local histone acetylation and transcriptional activation. A second class of non-HAT CREB coactivators, the CRTCs activate CREB independent of S133 phosphorylation (12–15). CRTCs are retained in the cytoplasm as a consequence of phosphorylation by AMPK family kinases, including salt-inducible kinases (SIKs) 1 and 2, and binding to 14-3-3 proteins (1). Cytoplasmic sequestration of CRTC2 is relieved by cAMP, which triggers PKA-dependent phosphorylation and inactivation of SIKs, and the actions of the Ca^{2+}-dependent phosphatase calcineurin, which dephosphorylates the inhibitor S171 residue on CRTC2 (15). Upon entering the nucleus, CRTCs bind the CREB bZIP domain and enhance both its DNA-binding activity and interaction with CBP (16–19). Although two-hit CREB activation by CBP and

*To whom correspondence should be addressed. Tel: +1 608 262 0027; Fax: +1 608 262 3913; Email: rstibbetts@wisc.edu

CRTC coactivators imparts signal specificity and robustness to CREB-mediated gene expression, it lacks inherent tunability. In addition, it remains unclear whether CREB DNA binding activity is autonomously regulated independent of CRTC tethering.

Work from our laboratory has focused on a cluster of conserved phosphorylation sites within the N-terminal portion of the CREB KID (S108, S111, S114, S117 and S121) that is coordinately phosphorylated by the apical DNA damage signaling kinase, ataxia-telangiectasia-mutated (ATM) and constitutively active CK1 and CK2 (20). ATM is a large molecular mass protein kinase best known for its critical participation in cell cycle checkpoint regulation and the signaling and repair of DNA double-strand breaks (DSBs) (21). Mutations in ATM cause ataxia-telangiectasia (A-T), a syndrome of cancer susceptibility and neurodegeneration in which sensitivity to ionizing radiation (IR) is a defining cellular characteristic. Genetic instability and cancer susceptibility in A-T are thought to arise from defects in cell cycle checkpoint regulation and DNA repair. However, other aspects of the A-T phenotype, including cerebellar neurodegeneration, metabolic syndrome and mitochondrial defects are more difficult to rationalize with known roles of ATM in DNA damage signaling (21–23).

ATM phosphorylates CREB in response to genotoxic stimuli through a processive phosphorylation mechanism (24). ATM-dependent phosphorylation of S111 primes the phosphorylation of S108 by CK2 and the phosphorylation of S114 and S117 by CK1. The phosphorylation of the upstream ATM and CK1/2 sites is required for phosphorylation of S121, which is restricted to conditions of moderate to severe DNA damage. Available evidence suggests that the ATM/CK cluster antagonizes CREB activity, potentially through destabilization of the CREB–CBP interaction (20); however, the physiologic impacts of ATM-mediated CREB phosphorylation remain to be determined and other biochemical roles for these modifications are possible. Finally, upstream CK1 and CK2 sites (S108, S111, S114 and S117) but not S121 are phosphorylated independent of ATM during cell growth (25); however, neither the upstream molecular signals nor functional consequences of this phosphorylation are understood.

Here we provide evidence that ATM/CK cluster phosphorylation influences CREB DNA binding activity and CRTC2 loading in a signal and phosphorylation stoichiometry-dependent manner. Under conditions of DNA damage, stoichiometric phosphorylation of CREB by ATM and CK1/2 led to its chromatin eviction and transcriptional attenuation. Paradoxically, substoichiometric phosphorylation of the ATM/CK cluster in response to cAMP contributed to maximal CREB activation and CRTC2 loading. Combined with the fact that mice expressing a non-phosphorylatable CREB allele exhibited both hypermorphic and hypomorphic CREB activity, these findings suggest a mechanism whereby graded phosphorylation of CREB tunes DNA binding and transcriptional output in response to changing environmental conditions.

MATERIALS AND METHODS

Mouse strains and glucagon injection

C57BL/6J-*CREB*$^{+/+}$ and C57BL/6J-*CREB*^{S111A} mice (homozygous for a Ser-111 to Ala mutation) were housed in colony cages with 12 h light/dark cycle in a temperature-controlled environment. About 8–12 week-old mice were injected with glucagon (200 μg/kg, i.p.; Sigma) or saline (control group). Livers were collected 1 h after injection and gene expression levels were determined. *CREB*$^{+/+}$ and *CREB*^{S111A} mice were placed on a high fat diet (HFD; Research Diets, Inc, D12492), which derived 60% of the caloric content from lard, for 17 weeks at weaning. Blood glucose was measured using a One Touch Ultra glucometer at week 16 of the HFD treatment, following a 16-h fast with cage change. Body weight and epididymal fat pad mass were measured in 20 week-old male mice, at the time of euthanasia.

Cell culture and reagents

Mouse embryonic fibroblasts (MEFs) were isolated from 14.5-day *CREB*$^{+/+}$ and *CREB*^{S111A} embryos. Where indicated, primary MEFs were immortalized by transfection with a plasmid encoding with SV40 large T antigen (p129; a gift from Dr Janet Mertz). Primary hepatocytes were isolated from *CREB*$^{+/+}$ and *CREB*^{S111A} 12-weeks female mice using the collagenase perfusion method. Primary MEFs, immortalized MEFs, primary hepatocytes, HeLa and HEK 293T cells were maintained in Dulbecco's modified Eagle's medium containing 10% fetal bovine serum and 1% penicillin-streptomycin. Forskolin (10 μM, Sigma) and IBMX (100 μM, Sigma) were treated for 90 min after serum starvation for overnight. PKA inhibitor H89 (10 μM, Sigma) and ATM inhibitor KU-55933 (10 μM, Sigma) were maintained in dimethyl sulfide (DMSO) and added to cells 30 min prior to stimulation. Calicheamicin A (CLM) was a kind gift of the Pfizer Compound Transfer Program and was maintained 4 μM stock solution in DMSO.

Microarray gene expression data analysis

Microarrays were carried out using Agilent SurePrint G3 Mouse Gene Expression 8 × 60K Microarray 8-plex slides ($n = 6$ embryos per genotype/per condition). RNA samples were labeled using the Agilent Low Input Quick Amp Labeling Kit, One-Color. Hybridizations were carried out using an Agilent Technologies DNA microarray model #G2565 CA. The pixel intensity data acquired from the microarrays were quantile normalized and log base 2 transformed. Since the arrays were processed at two different times (A and B), the data were corrected for this batch effect using ComBat and an empirical Bayes (26), non-parametric model of the data was performed with genotype and treatment as covariates. The data was then filtered by removing probes if 40 of the 48 arrays had values less than the fifth percentile and missing values subsequently imputed by flooring them at the fifth percentile. Differentially expressed genes were detected by analyzing the pre-processed data with a two-way MicroArray ANalysis Of Variance (MAANOVA) model (27,28) whereby genotype, treatment

and the interaction of the two were terms in the model. Contrasts (*t*-tests) between treated samples and their respective mock (untreated) controls were performed and *p*-values estimated from 1000 permutations of the samples being compared. Multiple comparisons correction was employed using the Benjamini and Hochberg procedure (29) and statistically significant differentially expressed genes selected based on an absolute fold change cut off of >1.5 and false discovery rate ≤ 0.05. Microarray data have been deposited in the NCBI Gene Expression Omnibus (GSE83891).

Quantitative RT-PCR

RNA analysis was carried out as described (30). The gene-specific primers for qPCR were used: mCREM (5′-TGATTCGCATAAACGTAGAGAAATTC-3′; 5′-CCATGGTAGCAATGTTAGGTGG-3′), mAREG (5′- CACCATAAGCGAAATGCCTTC-3′; 5′-TCTTGGGCTTAATCACCTGTTC-3′), mNR4A1 (5′-GCCTAGCACTGCCAACTTG-3′; 5′-TCTGCCCACT TTCGGATAAC-3′), mNR4A2 (5′- GCGGAGACTTTA GGTGCATGT-3′; 5′- TTGTTTATGTGGCTTGCGC-3′), mHAS2 (5′-CAGACAGGCGGAGGACGA-3′; 5′-AGAAACCTCTCACAATGCATCTTG-3′), mG6P (5′-TCACTTCTACTCTTGCTATCTTTCG-3′; 5′-CCCAGAATCCCAACCACAAG-3′), mPEPCK1 (5′-CCATCCCAACTCGAGATTCTG-3′; 5′-CTGAGGGCTTCATAGACAAGG-3′), mGAPDH (5′-GCCTTCCGTGTTCCTACC-3′; 5′-CCTCAGTGTAGCCCAAGATG-3′) and mPGK1 (5′-ACAGAGGATAAAGTCAGCCATG-3′; 5′-TTGACTTAGCACAGGAAC-3′).

Chromatin immunoprecipitation (ChIP)

Primary MEFs were cross-linked using 3% formaldehyde (Sigma) for 15 min, lysed and sonicated, and chromatin was immunoprecipitated with α-CREB (Millipore NL-904), α-CBP (Santa Cruz, SC-369) and α-CTRC2 (Calbiochem, ST1099) or α-rabbit IgG. After washing, the immunoprecipitated chromatin was reverse cross-linked and the liberated DNA fragments were purified using Qiagen spin columns. ChIP samples were measured by quantitative real-time polymerase chain reaction (PCR) using the CFX96 Touch™ Real-Time PCR Detection System (Bio-Rad) and SYBR Green. Primer sequences for the promoters: ChIP-mCREM (5′-TGCTAGTTCTTTCCTCCT GCC-3′; 5′-CTCGGAGCTGACGTCAATGT-3′), ChIP-mG6P (5′-GAGGCCTCCCAACATTCAT-3′; 5′-CTCA GAGCGTCTCGCCGGA-3′), ChIP-mPepck1 (5′- AGCC TTTGGTCAACAACTGG-3′; 5′-TGCCTTCGGGGTTA GTTATG-3′). The results were expressed as the relative fold occupancy of the target precipitation as compared to the input. HeLa cells expressed with FLAG-CREB^{WT}, CREB^{S114A}, CREB^{S117A}, CREB^{S121A} or CREB^{3A} were treated with/without 2 nM CLM for 1 h and then crosslinked with 1% formaldehyde for 10 min. After immunoprecipitated with α-FLAG (Sigma, F3165) antibodies, ChIP samples were measured by qPCR using primer sequences for the promoter: ChIP-hCREM (5′-CG CGTGTTATGGATGTTTGTGTGCCT-3′; 5′-GGAACT GACTAAATCACAACATGACTCGGA-3′). The relative FLAG-CREB occupancy on the CREM promoter (Figure 4A) was calculated as a ratio of promoter occupancy in the presence or absence of CLM.

Chromatin fractionation

Chromatin fractionation of cells was modified from our previous publication (31). MEFs, HeLa or HEK 293T cell pellets derived from ∼5 × 10^6 cells were separated to nuclear/cytoplasmic fractions using cytoplasm extraction buffer (10 mM HEPES, 60 mM KCl, 1 mM ethylenediaminetetraacetic acid, 0.1% NP40, 1 mM DTT and 1 mM PMSF). The nuclear fractions were extracted with CSK buffer (10 mM PIPES, 100 mM NaCl, 300 mM sucrose, 1 mM $MgCl_2$, 1 mM DTT, 1 mM EGTA, 0.1% Triton X-100) with protease and phosphatase inhibitors, and centrifuged at 3000 × *g* for 10 min. The supernatant was collected as the nuclear soluble protein fraction. The remaining cell pellets (chromatin) were washed once with CSK buffer and then boiled in sample loading buffer prior to analysis by sodium dodecyl sulphate-polyacrylamide gel electrophoresis (SDS-PAGE).

Electrophoretic mobility shift assay (EMSA)

The double-stranded oligonucleotides CRE-Forward: 5′-GATCTGCGTCAGAGT-3′ and CRE-Reverse: 5′-ACTCTGACGCAGATC-3′ were labeled with [α-^{32}P] dATP and polynucleotide kinase. Cell lysates or purified CREB proteins were incubated with the probe in a buffer containing 10 mM Tris (pH 7.5), 50 mM KCl, 1 mM DTT, 7.5% glycerol and 75 ng/μl poly(dI-dC) for 20 min at room temperature. The reaction mixture was separated with 6% native polyacrylamide gel. The [^{32}P]-labeled protein–DNA complexes were visualized by autoradiography.

Recombinant DNA and protein analysis

Gal4-CREB (pFA2-CREB; Agilent) encodes the 147 amino acids Gal4 DNA-binding domain fused to CREB amino acids 1–280. KCREB was a gift from Dr Richard Goodman. GFP-CREB (249-341) and GFP-CREB (282–341) were subcloned into pQCXIN for GFP-Q2-bZIP and GFP-bZIP, respectively. 6×-His-CREB 1–197 was generated by digesting full-length CREB:pET-28a with KpnI followed by Klenow end polishing and religation. The GST-CRTC2^{CBD} plasmid was a kind gift of Dr Marc Montiminy and has been described (12). FLAG-CREB expression plasmids in pFLAG-CMV and pcDNA3.1-based vectors have been described (20,24,25). Purified CREB protein was a kind gift from Dr Jennifer Nyborg (Colorado State University). Protein was extracted from cultured cells in high salt lysis buffer (25 mM HEPES (pH 7.4), 300 mM NaCl, 1.5 mM $MgCl_2$, 1 mM EGTA, 0.1% Triton X-100) supplemented with protease inhibitors and phosphatase inhibitors for 10 min on ice and proteins were separated on a SDS-PAGE. Antibodies used in this study include: α-pCREB-Ser-108/Ser-111/Ser-114 (24), α-pCREB-Ser-121 (20), α-pCREB-Ser-133 (Millipore 06–519 and Cell Signaling 87G3), α-FLAG (Sigma F7425), α-FUS (Santa

Cruz 4H11), α-MCM3 (Bethyl laboratory A300-192A), α-Gal4 (Santa Cruz RK5C1), α-GFP (Santa Cruz B-2), α-β-tubulin (Millipore AA2) and α-HSP90 (Cell Signaling C45G5).

RESULTS

CREB is phosphorylated on CK1/2 sites in response to cAMP

Previous work from our laboratory established that the ATM/CK cluster is processively phosphorylated by ATM and CK1/2 in response to DNA damage and phosphorylated independent of DNA damage and ATM during cell growth (20,24,25) (Figure 1A); however, the upstream signals controlling DNA damage-independent CREB phosphorylation are not known. During the course of experiments using the adenylate cyclase agonist forskolin (Fsk) we noticed that CREB isolated from MEFs treated with Fsk exhibited an electrophoretic mobility shift highly characteristic of ATM/CK cluster phosphorylation (Figure 1B). Immunoblotting with an antibody that detects CREB triply phosphorylated on S108, S111 and S114 (α-CREB-pS108/111/114) confirmed these residues were phosphorylated upon Fsk exposure. Although ATM phosphorylates CREB on S111 in response to IR (20), the ATM inhibitor KU-55933 had no impact on S111 phosphorylation by Fsk (Figure 1B). On the other hand, Fsk did not induce immunoreactivity with an antibody that detects CREB phosphorylated on S121, which is consistent with our previous findings that phosphorylation of this site is DNA damage dependent (data not shown). Fsk-induced CREB S111 phosphorylation was observed within 30 min of treatment and was blocked by the PKA inhibitor, H-89 (Figure 1C, top and middle panels). Thus, even though S111 is not a consensus PKA site and is unlikely to be directly phosphorylated by PKA, PKA activity is upstream of S111 phosphorylation in response to Fsk. One possibility that could account for these findings is that phosphorylation of CREB on S133 renders it more susceptible to phosphorylation by CK1/2, which are abundant and constitutively active kinases. Arguing against this, however, Fsk-induced phosphorylation of the ATM/CK cluster comparably between $CREB^{+/+}$ MEFs and $CREB^{S133A}$ MEFs generated by Naqvi *et al.* (32) (Supplementary Figure S1). We conclude that cAMP-induced phosphorylation of the ATM/CK cluster occurs downstream of PKA but independent of S133 phosphorylation.

cAMP-induced CREB phosphorylation requires a functional DNA-binding domain

We used transiently expressed CREB proteins to explore determinants of CREB phosphorylation by cAMP. Interestingly, a R301L mutation (KCREB) that abolishes CREB DNA binding diminished constitutive and Fsk-induced phosphorylation of S111 in HEK 293T cells (Figure 1D), whereas DNA damage-induced phosphorylation of KCREB was largely intact. A $CREB^{Q321A}$ mutant that retains partial DNA binding activity but is defective for CRTC2 binding (16) exhibited an intermediate S111 phosphorylation phenotype (Figure 1D). On the other hand, a C-terminal fusion of CREB to the Gal4 DNA binding domain (Gal4-CREB) showed high levels of both S111 and S121 phosphorylation when expressed in HEK 293T cells even though it lacks a bZIP domain. Thus, DNA binding activity—but not CRE-specific DNA binding—is required for maximal CREB phosphorylation on CK1/2 sites in cells.

To further investigate the relationship between DNA binding and phosphorylation we examined the effect of ds-DNA oligonucleotides on CREB phosphorylation by CK1 *in vitro*. Oligonucleotides containing or lacking an embedded CRE stimulated the CK1-dependent phosphorylation of CREB on the ATM/CK cluster *in vitro*. The stimulation of CREB phosphorylation by CK1 was DNA concentration dependent and most pronounced for the S121 phosphorylation site (Figure 1E and F). We conclude that targeting to DNA increases the phosphorylation of CREB by CK1/2 *in cellulo* and that binding to DNA increases the intrinsic phosphorylation potential of recombinant CREB *in vitro*.

CREB S111 phosphorylation inhibits or enhances CREB target gene expression in a signal dependent manner

To further explore the physiologic relevance of ATM/CK cluster phosphorylation in response to activating and stress stimuli, we introduced a Ser-111 to Ala knock-in mutation into the mouse germ line that abolishes phosphorylation of the ATM/CK cluster (24) (Supplementary Figure S2). Homozygous $CREB^{S111A/S111A}$ ($CREB^{S111A}$) knock-in mice were indistinguishable in appearance or activity level from wild-type (WT) littermates. As predicted from previous studies, IR-induced phosphorylation of S121 was undetectable in $CREB^{S111A}$ splenocytes (Figure 2A) and the characteristic IR-induced electrophoretic mobility shift of CREB due to phosphorylation of CK1/2 sites at S108, S111, S114 and S117, was abolished. Fsk-induced phosphorylation of the ATM/CK cluster was also abolished in $CREB^{S111A}$ MEFs (Figure 2B). Finally, given previous work showing that DNA damage-induced phosphorylation of S111 inhibited CREB interaction with the KID-interacting (KIX) domain of CBP (20,24) we tested binding of CREB to a GST-KIX domain fragment in pull-down assays. We found that $CREB^{S111A}$ from spleen extracts bound to the CBP KIX domain more strongly than did $CREB^{WT}$. IR had a small but reproducible inhibitory effect on the $CREB^{WT}$/KIX domain interaction, whereas $CREB^{S111A}$ binding to KIX was completely resistant to IR (Figure 2C).

Microarray experiments were employed to examine the effects of the S111A mutation on CREB target gene expression in MEFs treated with IR, Fsk or Fsk preceded by IR. The top 50 Fsk-induced genes and their expression under the IR-Fsk condition in $CREB^{+/+}$ and $CREB^{S111A}$ MEFs are shown in Supplementary Table S1A and B. The majority of Fsk-induced genes in $CREB^{+/+}$ MEFs showed reduced expression when Fsk was preceded by IR, whereas the same CREB target genes were, for the most part, not attenuated in IR-Fsk-treated $CREB^{S111A}$ MEFs (Table 1). Guided by a publication from Brindle and colleagues (33), we used qPCR to query expression of CBP/p300-dependent and

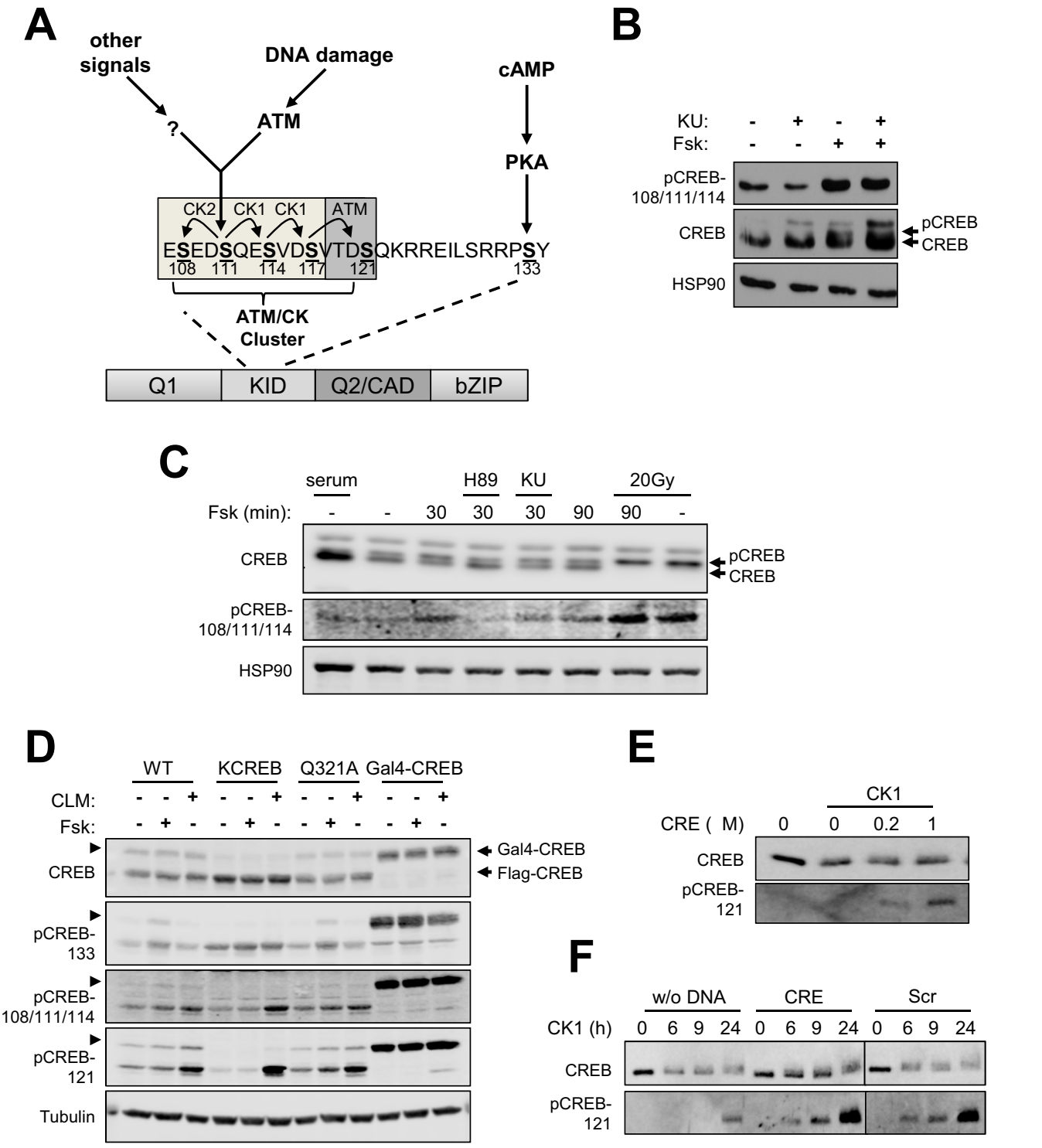

Figure 1. cAMP-induced phosphorylation of the CREB ATM/CK cluster. (**A**) Schematic depiction of the CREB ATM/CK phosphorylation cluster. (**B**) *CREB*$^{+/+}$ MEFs were pretreated with KU-55933 (KU) for 30 min and then the cells were treated with Fsk for 90 min. Cell extracts were immunoblotted with α-pCREB-108/111/114, α-CREB or α-HSP90 antibodies. (**C**) *CREB*$^{+/+}$ MEFs were pretreated with either H-89 (PKA inhibitor), KU-55933 (ATM inhibitor) or 20 Gy IR followed by Fsk for 30 or 90 min. Cell extracts were analyzed using α-CREB, α-pCREB-108/111/114 or α-HSP90 antibodies. (**D**) Phosphorylation of CREB was analyzed by western blotting using cell lysates prepared from HEK 293T cells transfected with plasmids encoding CREB^{WT}, KCREB, CREB^{Q321A} (CRTC2 binding mutant) or Gal4-CREB. The transfected cells were treated with Fsk or 2 nM CLM for 60 min. CREB expression and phosphorylation were determined by immunoblotting with indicated antibodies. Arrowheads (lane 1–9) indicate presumed Sumo-CREB detected by CREB antibodies. (**E**) Recombinant CREB was incubated with CK1 and ATP with the indicated amount of CRE oligonucleotide. CREB phosphorylation was analyzed by western blotting using α-CREB or α-pCREB-121 antibodies. (**F**) Recombinant CREB was phosphorylated with CK1 in the presence or absence of CRE or scrambled DNA (Scr) for the indicated times. CREB phosphorylation was analyzed by western blotting using α-CREB or α-pCREB-121 antibodies.

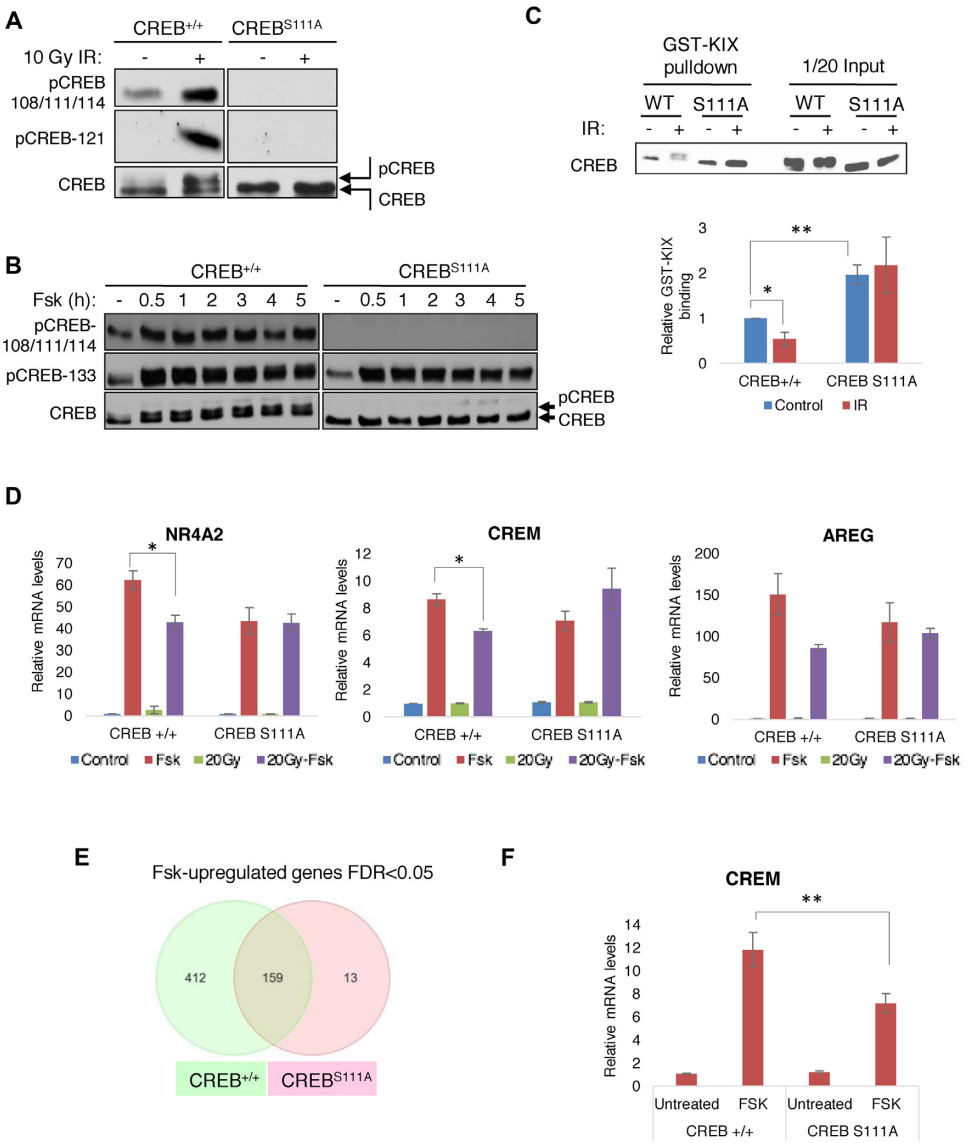

Figure 2. ATM/CK cluster positively and negatively regulates CREB transcriptional activity. (**A** and **B**) A Ser-111 to Ala knock-in mutation abolishes ATM/CK cluster phosphorylation in response to DNA damage (A) and Fsk (B). In panel (A) e*x vivo* cultured splenocytes were sham treated or exposed to 10 Gy IR and cell extracts were prepared 1 h later for western analysis using the indicated antibodies. In panel (B) $CREB^{+/+}$ and $CREB^{S111A}$ MEFs were treated with 10 μM Fsk and the cells were collected at the indicated times. Cell extracts were immunoblotted with α-pCREB-108/111/114, α-pCREB-133 or α-CREB antibodies. (**C**) $CREB^{S111A}$ protein exhibited increased affinity for the CBP KIX domain. GST-KIX pull-downs were performed using spleen extracts from $CREB^{+/+}$ or $CREB^{S111A}$ mice before or after 10 Gy irradiation. GST-KIX binding activity was measured by densitometric analysis. $n = 4$. (**D**) DNA damage-resistant gene expression in $CREB^{S111A}$ MEFs. $CREB^{+/+}$ and $CREB^{S111A}$ MEFs were treated as in (**E**) and levels of indicated genes determined by qPCR. Each bar represents averaged results for three biological replicates, assayed three times each. (E) Fsk-inducible genes in $CREB^{+/+}$ and $CREB^{S111A}$ MEFs determined by microarray analysis. (**F**) Defective cAMP-induced expression of CREM in $CREB^{S111A}$ MEFs. $CREB^{+/+}$ and $CREB^{S111A}$ MEFs were treated with Fsk for 90 min and CREM mRNA expression analyzed by qPCR. Each bar represents averaged results, $n = 24$. Data information: **i**n (C–F), data are presented as mean ± SEM. $*P < 0.05$, $**P < 0.02$ (Student's *t*-test).

CBP/p300-independent CREB target genes in $CREB^{+/+}$ and $CREB^{S111A}$ MEFs, reasoning that the former set of genes may be most sensitive to DNA damage and the S111A mutation. The Fsk-induced expression of both CBP/p300-dependent (AREG) and CBP/p300-independent (CREM, NR4A2) was attenuated by IR and, in all instances, attenuation failed to occur in $CREB^{S111A}$ MEFs (Figure 2D). Similar findings were made for additional CBP-dependent and CBP-independent CREB target genes (Supplementary Figure S3). Thus, IR attenuates CREB-mediated gene expression in a Ser-111 phosphorylation-dependent manner; however, because this occurred for both CBP-dependent and CBP-independent genes, diminution of CBP/p300 binding is not the major mechanism through which this occurs.

The above findings supported an inhibitory role for the ATM/CK cluster in CREB transcriptional activation following IR exposure. Surprisingly, however, a comparison of the MEF microarray data revealed the opposite trend

Table 1. Relative attenuation of Fsk-induced genes by IR in CREB$^{+/+}$ and CREB^{S111A} MEFs

Gene symbol	CREB $^{+/+}$ Fold change (log_2) Fsk and IR versus Fsk_only and IR only	CREB ^{S111A} Fold change (log_2) Fsk and IR versus Fsk_only and IR_only
Junb	−1.99482	1.13155
Areg	−1.80694	−1.21135
Il6	−1.80623	−1.16726
Gem	−1.73148	−1.02846
Scrt1	−1.72122	−1.07231
Nefl	−1.70273	−1.10401
Crem	−1.68828	1.0897
Adrb1	−1.55724	−1.06747
Ier3	−1.54472	1.23746

in the context of cAMP signaling, where 571 and 172 genes were significantly upregulated by Fsk in *CREB*$^{+/+}$ and *CREB*^{S111A} MEFs, respectively (Figure 2E). Consistent with a mild activation defect, qPCR experiments revealed blunted CREM induction by Fsk in *CREB*^{S111A} MEFs, with similar findings made for other CREB target genes (Figure 2F and Supplementary Figure S4A). As a whole, fewer genes were significantly upregulated by Fsk in *CREB*^{S111A} MEFs versus *CREB*$^{+/+}$ MEFs, supporting the notion that Fsk-inducible gene expression was slightly compromised by the S111A mutation (Supplementary Figure S4B). Thus, ATM/CK cluster phosphorylation attenuates target gene expression in the context of DNA damage but paradoxically contributes to maximal gene expression in response to cAMP.

S111 dependence of CREB target genes correlates with CRTC2 occupancy

We next sought to determine the underlying mechanisms for S111 phosphorylation-dependent changes in CREB-mediated transcription. ChIP assays were performed to measure the occupancy of CREB and its coactivators, CBP and CRTC2 over CREB target genes in *CREB*$^{+/+}$ and *CREB*^{S111A} MEFs before and after DNA damage. Fsk exposure increased CBP occupancy over *AREG* and *CREM/ICER* promoters in *CREB*$^{+/+}$ MEFs (Figure 3A and Supplementary Figure S5A); however, CBP recruitment was not significantly inhibited by IR, suggesting that either CBP is not the critical target of DNA damage-dependent regulation or that the CBP ChIP assay lacks sufficient dynamic range to reveal such differences. On the other hand, Fsk-dependent recruitment of CRTC2 to CREM and AREG was reduced in an S111 phosphorylation-dependent manner upon irradiation (Figure 3A and Supplementary Figure S5A). CRTC2 recruitment to CREM was also reduced in immortalized *CREB*$^{+/+}$ MEFs, but not *CREB*^{S111A} MEFs treated with the radiomimetic agent CLM (Supplementary Figure S5B). Reductions in CRTC2 promoter recruitment could be caused by defects in its nuclear translocation; however, CRTC2 nuclear accumulation was comparable between *CREB*$^{+/+}$ and *CREB*^{S111A} MEFs treated with Fsk in the absence or presence of CLM (Supplementary Figure S6A and B). Finally, ChIP experiments also revealed that Fsk-induced CRTC2 recruitment to CREM was significantly lower in *CREB*^{S111A} MEFs than *CREB*$^{+/+}$ MEFs (Figure 3A). The reduced recruitment of CRTC2 plausibly explains the blunted induction of CREB target genes in *CREB*^{S111A} MEFs.

The CREB bZIP binds to the CREB-binding domain (CBD) of CRTC2 to form a ternary complex with enhanced DNA-binding activity (12,16). To investigate the effects of DNA damage and ATM/CK cluster phosphorylation on CREB–CRTC2–DNA ternary complexes, we incubated cell extracts from control or CLM-treated HEK 293T cells expressing CREB^{WT} or a non-phosphorylatable CREB^{3A} mutant harboring Ala mutations at Thr-100, Ser-111 and Ser-121 with recombinant GST-CBD and dsDNA oligonucleotides with or without an embedded CRE. Consistent with previous findings (16), the interaction of GST-CBD and CREB was enhanced by dsDNA, and CRE-containing DNA fragments stimulated interaction to a greater extent than those lacking a CRE (Figure 3B). Under conditions of isotonic NaCl, CREB^{WT} and CREB^{3A} interacted comparably with GST-CBD/DNA and cellular exposure to CLM had little effect on the interaction. However, ternary complexes containing phosphorylated CREB^{WT} but not CREB^{3A}, were dissociated upon washing with buffer containing 300 mM NaCl (Figure 3B). Thus, DNA damage disrupts CREB–CRTC2–DNA ternary complexes in a phosphorylation-dependent manner.

DNA damage-induced phosphorylation of the ATM/CK cluster inhibits CREB DNA-binding activity

Because CRTC2 binding is stimulated by CREB interaction with DNA, it was possible that DNA damage-dependent reductions in CREB–CRTC2–DNA ternary complexes occurred secondary to reduced association of CREB with DNA. To investigate this we performed electrophoretic mobility shift assays (EMSA) using extracts prepared from *CREB*$^{+/+}$ and *CREB*^{S111A} MEFs. CLM exposure also reduced CREB DNA binding affinity in *CREB*$^{+/+}$ MEFs but not *CREB*^{S111A} MEFs, supporting the notion that ATM-mediated phosphorylation of the ATM/CK cluster reduces CREB DNA-binding affinity (Figure 3C). DSB inducers etoposide and camptothecin also reduced CREB DNA binding affinity in *CREB*$^{+/+}$ MEFs but not *CREB*^{S111A} MEFs (Supplementary Figure S7).

We also performed EMSA using extracts prepared from HEK 293T cells transiently transfected with plasmids encoding WT and mutant CREB cDNAs. Binding of CREB^{WT} to a double-stranded oligonucleotide probe containing a CRE half-site was reduced following exposure of HEK 293T cells to IR whereas the binding of non-

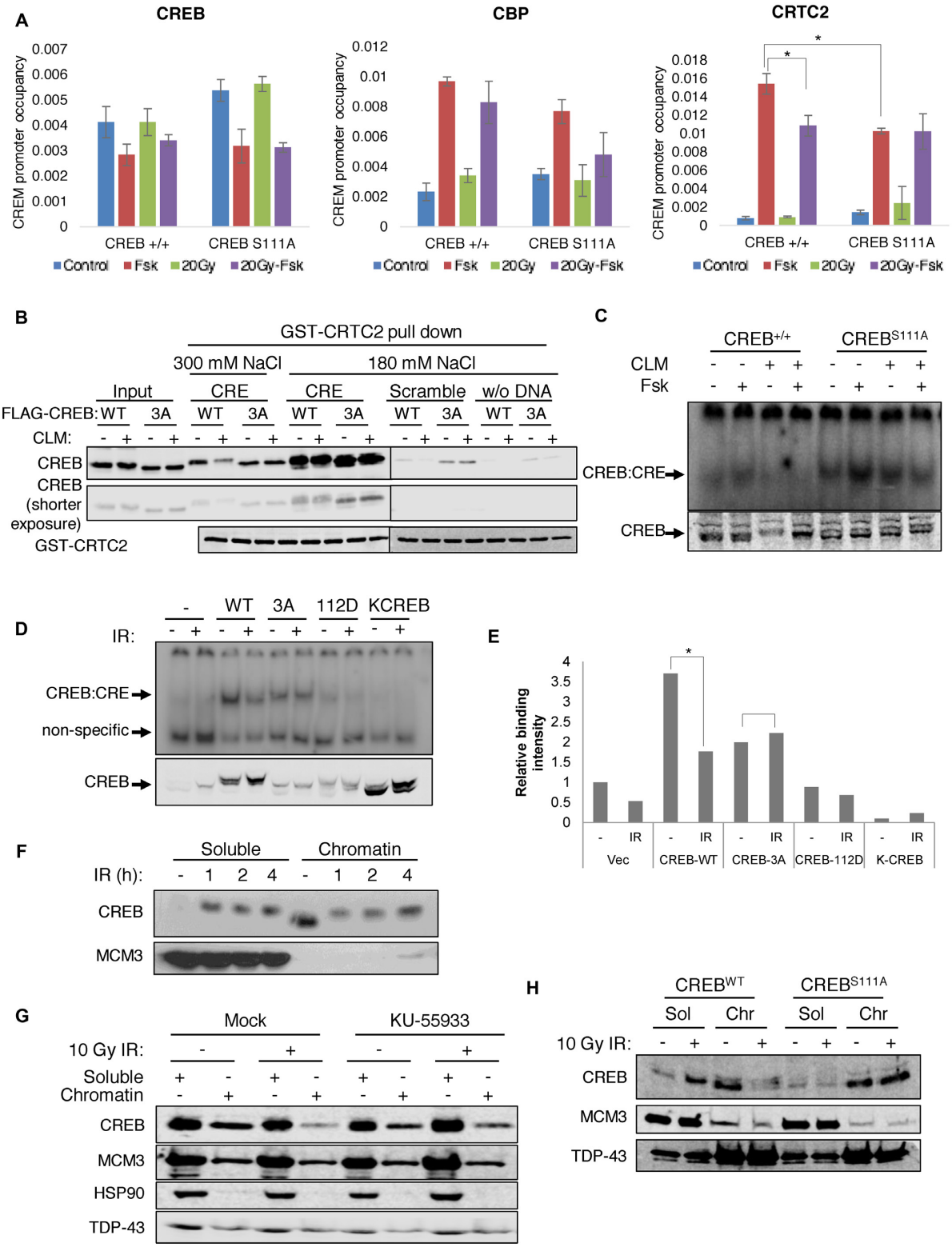

Figure 3. Impact of DNA damage and CREB S111 phosphorylation on coactivator recruitment and DNA binding activity. (**A**) ChIP analysis of CREB, CBP and CRTC2 over the CREM promoter in *CREB*$^{+/+}$ and *CREB*^{S111A} MEFs. Cells were treated with Fsk for 90 min, irradiated with 20 Gy IR for 120 min (20 Gy) or treated with 20 Gy IR 30 min prior to Fsk (20 Gy-Fsk) and processed for ChIP-qPCR using the indicated antibodies. Y-axis represents the CREM promoter occupancy. Each bar represents averaged results, $n = 3$. Error bars indicate SEM. $*P < 0.05$ (Student's t-test). (**B**) DNA damage inhibits CREB–CRTC2–DNA ternary complex formation in an S111 phosphorylation-dependent manner. HEK 293T cells transfected with CREB^{WT} or CREB^{3A} were treated with 2 nM CLM for 1 h and cell lysates incubated with GST-CRTC2^{CBD} and either CRE-containing or scrambled oligonucleotides in the presence of GSH-agarose beads. Immobilized CREB–CRTC2–DNA ternary complexes were washed under indicated buffer conditions analyzed by

phosphorylatable CREB^{3A} was unaffected (Figure 3D and E). A CREB^{Q112D} mutant that exhibits a reduced threshold for DNA damage-dependent phosphorylation (24) bound weakly to the probe and its binding was further reduced upon DNA damage. A DNA-binding defective CREB^{R301L} 'KCREB' mutant (34), failed to bind the CRE probe in these experiments. Finally, we observed a strong decrease in CREB chromatin association following DNA damage (Figure 3F). IR-dependent CREB chromatin dissociation was partially suppressed by the ATM inhibitor KU-55933 and was abolished by the S111A mutation (Figure 3G and H). From the combined EMSA and chromatin fractionation studies we conclude that DNA damage-induced phosphorylation of the ATM/CK cluster diminishes affinity for DNA.

The ATM/CK cluster functions as a DNA binding rheostat

Multisite phosphorylation domains can function as molecular switches (35) to mediate on-off responses to threshold stimuli, or as molecular rheostats to impart graded biochemical behavior proportional to the number of phosphoresidues (36). To investigate whether the ATM/CK cluster operates as a switch or rheostat we carried out ChIP experiments using an allelic series of CREB phospho-site mutants, which owing to the processive nature of phosphorylation (24), generate predictable phosphorylation intermediates upon DNA damage. Because initial ChIP experiments in Figure 3A did not reveal different occupancy patterns between endogenous CREB^{WT} and CREB^{S111A} in MEFs, we employed milder formaldehyde crosslinking conditions to reduce handcuffing artifacts that may mask dynamic CREB–DNA interactions. We found that DNA damage reduced CREB occupancy of the CREM promoter, with the magnitude of dissociation roughly correlating with predicted CREB phosphorylation stoichiometry. CREB^{WT} (five phosphorylated residues, or 5P), showed maximal dissociation from the CREM promoter following CLM, whereas CREB^{3A} (no phosphorylated residues or 0P) was completely resistant to CLM (Figure 4A). CREB^{S114A} (2P), CREB^{S117A} (3P) and CREB^{S121A} (4P), showed intermediate levels of dissociation following CLM treatment, with CREB^{S121A} behaving similar to CREB^{WT}. These findings suggest that ATM/CK cluster phosphorylation inhibits CREB DNA binding activity in graded fashion proportional to the number of phosphate groups.

The same allelic series of CREB phosphosite mutants was tested for ternary complex formation in the presence of GST-CBD and dsDNA. As expected, CLM treatment inhibited the interaction between CREB^{WT} and GST-CBD, but had essentially no effect on the interaction between CREB^{3A} and GST-CBD (Figure 4B and C). Binding of GST-CBD to CREB^{S114A}, CREB^{S117A} and CREB^{S121A}, showed intermediate responsiveness to CLM, with the more heavily phosphorylated CREB^{S121A} isoform exhibiting the lowest affinity. Combined with the ChIP findings, these results indicate that the multisite phosphorylation of the ATM/CK cluster imparts graded behavior, as opposed to switch-like properties, to CREB DNA binding and CRTC ternary complex formation.

We next considered how phosphorylation of the distal ATM/CK cluster, which resides in N-terminal portion of the unstructured KID, might modulate CREB DNA binding activity and CREB–CRTC2–DNA ternary complex formation. One possibility was that the hyperphosphorylated ATM/CK cluster competes with the phosphate backbone of DNA for binding to basic residues within the bZIP. To test this we carried out pull-down experiments using a purified, truncated form of His-CREB lacking the bZIP domain (CREB 1–197) and GFP-bZIP-domain fragments (see methods) that had been expressed in HEK 293T cells. As shown in Figure 4D, His-CREB 1–197 interacted with a GFP-tagged CREB fragment containing the bZIP and a portion of the adjacent Q2 domain (Q2-bZIP) but not a minimal GFP-bZIP. Thus, the isolated amino terminal and Q2-bZIP domains interact; however, attempts to phosphorylate CREB 1–197 with CK1/2 *in vitro* were unsuccessful, possibly because phosphorylation requires a functional DNA binding domain (Figure 1D). To work around this difficulty we employed the Gal4-CREB construct that undergoes robust phosphorylation of the ATM/CK cluster in intact cells (Figure 1D). Gal4-CREB interacted with the GFP-bZIP in co-IP assays, however the interaction was not affected by CLM treatment (Figure 4E). We conclude that CREB is capable of intramolecular association; however, the interaction appears to occur both in the absence and presence of ATM/CK cluster phosphorylation.

CREB S111 phosphorylation contributes to the regulation of gluconeogenic genes

During fasting, CREB works in conjunction with FOXO TFs in the liver to induce gluconeogenic gene expression in response to the peptide hormone glucagon (37). To examine whether ATM/CK cluster phosphorylation modulates CREB-dependent expression of gluconeogenic genes we measured hepatic glucose-6 phosphatase (G6P) and PEPCK expression *CREB*$^{+/+}$ and *CREB*^{S111A} mice fol-

←

western blotting with α-CREB and α-GST antibodies. (**C**) Immortalized *CREB*$^{+/+}$ and *CREB*^{S111A} MEFs were treated with Fsk for 90 min, treated with 2 nM CLM for 120 min (CLM), or treated with CLM for 30 min prior to Fsk (CLM + Fsk). CREB–CRE complexes were analyzed by electrophoretic mobility shift assay (EMSA). (**D**) DNA-binding activity was analyzed by EMSA using cell lysates prepared from HEK 293T cells transfected with empty vector, or plasmids encoding CREB^{WT}, CREB^{3A} (100A, 111A and 121A), CREB^{Q112D} or DNA-binding defective KCREB. The transfected cells were irradiated with 50 Gy IR for 1 h and CREB expression analyzed by immunoblotting. (**E**) CRE binding activity was measured by densitometric analysis. *$P < 0.05$ (Student's *t*-test). (**F**) DNA damage caused dissociation of CREB from bulk chromatin. HeLa cells were irradiated with 10 Gy IR, collected at the indicated times, and fractionated into soluble (Sol) or chromatin (Chr) fractions prior to sodium dodecyl sulphate-polyacrylamide gel electrophoresisand immunoblotting with α-CREB or α-MCM3 antibodies. (**G**) CREB chromatin dissociation is ATM dependent. HeLa cells were pretreated with DMSO or ATM inhibitor (KU-55933) for 30 min, and then irradiated with 10 Gy IR for 1 h. Soluble (Sol) or chromatin (Chr) fractions were analyzed using α-CREB, α-HSP90, α-MCM3 or α-TDP-43 antibodies. (**H**) The S111A mutation inhibits IR-dependent CREB chromatin eviction. Chromatin fractionation of *CREB*$^{+/+}$ and *CREB*^{S111A} MEFs was carried out 1 h after irradiation of 10 Gy IR.

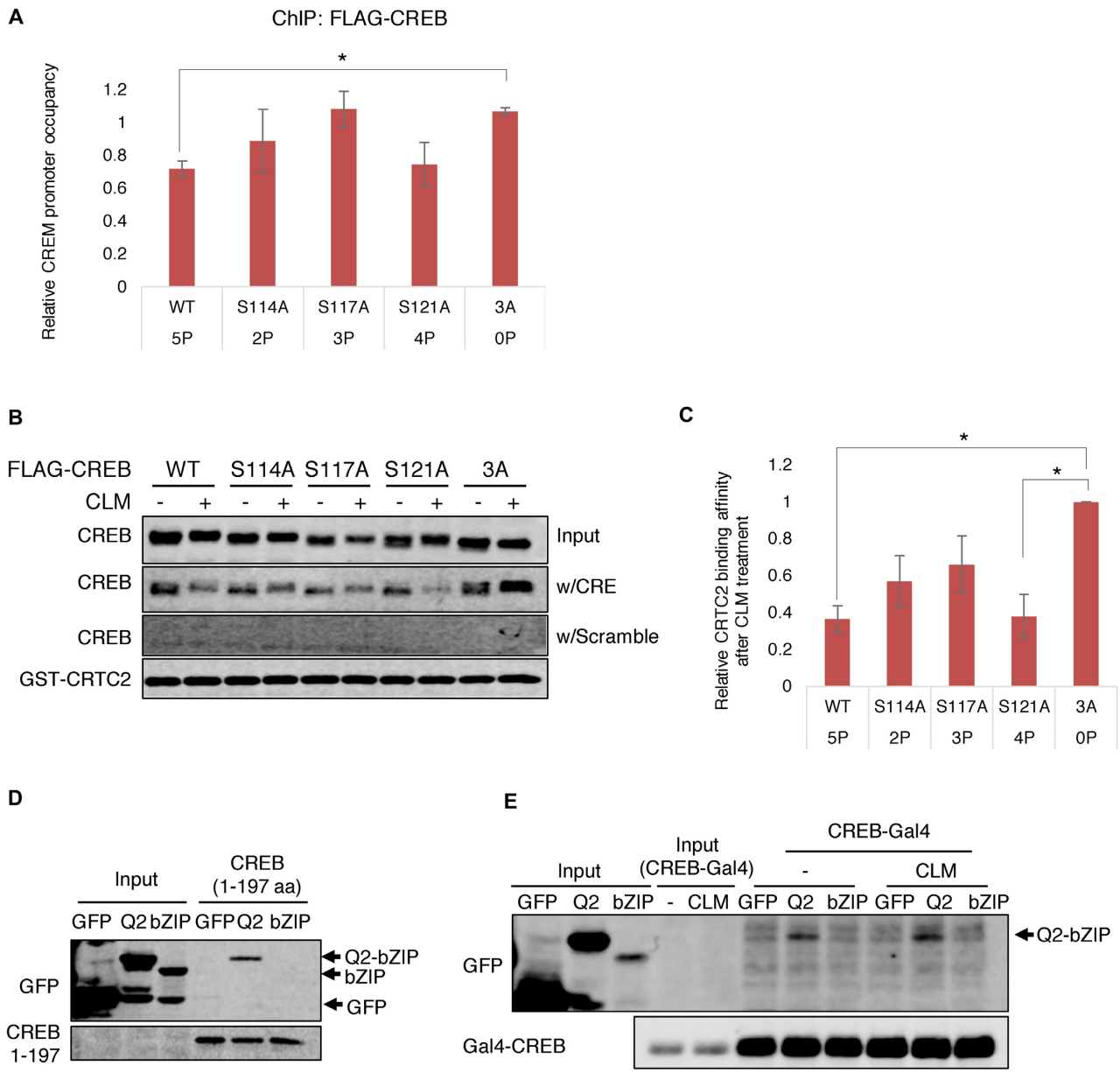

Figure 4. Phosphorylation of the ATM/CK cluster inhibits DNA binding and CREB–CRTC2–DNA ternary complex formation in graded fashion. (**A**) ChIP analysis of CREB phosphosite mutants. HeLa cells transfected with FLAG-tagged $CREB^{WT}$, $CREB^{S114A}$, $CREB^{S117A}$, $CREB^{S121A}$ or $CREB^{3A}$ were treated with 2 nM CLM for 1 h and subjected to ChIP-qPCR using α-FLAG antibodies and primers spanning the CREB binding site in the *CREM/ICER* promoter. $*P < 0.05$ (Student's *t*-test). (**B**) Effects of CREB phosphosite mutations on CREB–CRTC2–DNA ternary complex formation. HEK 293T cells transfected with $CREB^{WT}$, $CREB^{S114A}$, $CREB^{S117A}$, $CREB^{S121A}$ or $CREB^{3A}$ were treated with 2 nM CLM for 1 h and cell lysates incubated with GST-$CRTC2^{CBD}$ and either CRE-containing or scrambled oligonucleotides in the presence of GSH-agarose beads. Immobilized CREB–CRTC2–DNA ternary complexes were washed under indicated buffer conditions analyzed by western blotting with α-CREB and α-GST antibodies. (**C**) Densitometric analysis of CREB binding to GST–$CRTC2^{CBD}$–DNA complexes. $*P < 0.05$ (Student's *t*-test). (**D**) Intramolecular interaction between Q2-bZIP and amino-terminal regions of CREB. Recombinant 6×-His-CREB lacking the bZIP domain (CREB 1–197) was incubated with cell lysates from HEK 293T cells transfected with GFP or GFP fused to a minimal CREB bZIP domain (GFP-bZIP) or an extended bZIP domain containing a portion of the adjacent Q2 domain (GFP-Q2-bZIP). The 6×- His tag pull-downs were analyzed by immunoblotting with α-GFP antibody. (**E**) Interaction between Gal4-CREB and Q2-bZIP is unaffected by DNA damage. GFP, GFP-Q2-bZIP or GFP-bZIP were immunoprecipitated (IP) from transfected HEK 293T cells with α-GFP antibody. The IP samples were incubated with cell lysates from HEK 293T cells separately transfected with Gal4-CREB with or without treatment of 2 nM CLM. Co-immunoprecipitated proteins were analyzed by western blotting with α-GFP or α-CREB antibodies.

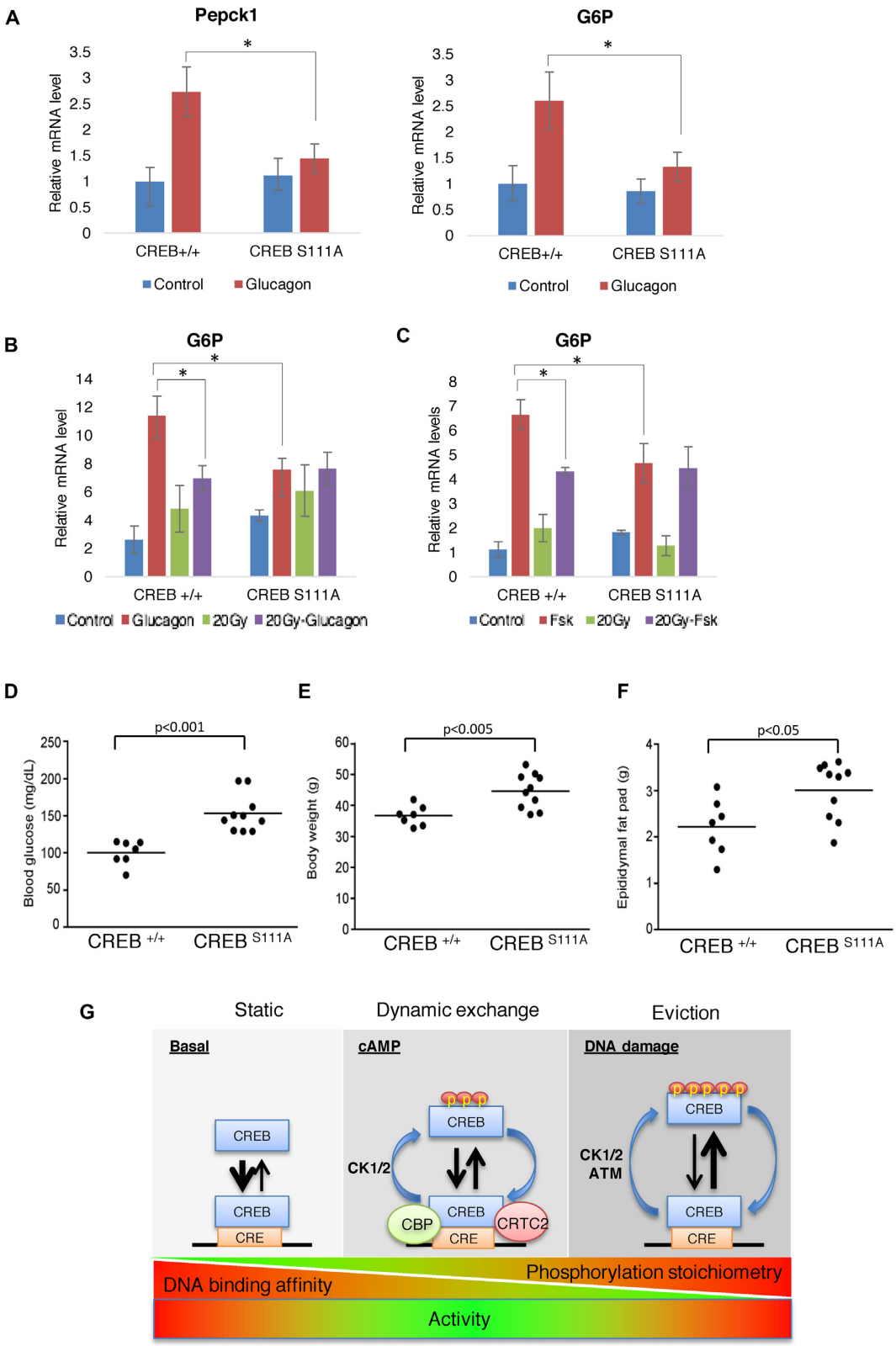

Figure 5. CREB S111 phosphorylation contributes to the bidirectional regulation of gluconeogenic genes by cAMP and IR *in vivo*. (**A**) $CREB^{+/+}$ and $CREB^{S111A}$ mice were injected with either PBS or 200 μg/kg glucagon and expression levels of G6P and PEPCK at 1 h analyzed by qPCR. Each bar represents averaged results for three biological replicates, assayed three times each. Error bars indicate SEM $*P < 0.02$ (Student's *t*-test). (**B**) $CREB^{+/+}$ and $CREB^{S111A}$ primary hepatocytes were treated with glucagon for 60 min, irradiated with 20 Gy IR for 120 min (20 Gy) or treated with glucagon for 60 min after 20 Gy IR for 30 min (20 Gy-glucagon). $*P < 0.05$ (Student's *t*-test). (**C**) $CREB^{+/+}$ and $CREB^{S111A}$ primary hepatocytes were treated with Fsk for

lowing intraperitoneal injection with glucagon. Glucagon-induced expression of hepatic G6P and PEPCK were attenuated in $CREB^{S111A}$ mice versus $CREB^{+/+}$ mice (Figure 5A), suggesting that S111 phosphorylation is required for maximal induction of gluconeogenic CREB target genes *in vivo*. To extend these findings we measured G6P expression in $CREB^{+/+}$ and $CREB^{S111A}$ hepatocytes under conditions of DNA damage and in response glucagon. Preexposure to IR attenuated glucagon-induced expression of G6P in $CREB^{+/+}$ hepatocytes, but not $CREB^{S111A}$ hepatocytes, with similar findings made for Fsk (Figure 5B and C), supporting an inhibitory role for ATM/CK cluster phosphorylation in the context of these gluconeogenic genes. On the other hand, and consistent with studies using MEFs, Fsk-induced level of G6P was lower in $CREB^{S111A}$ hepatocytes relative to $CREB^{+/+}$ hepatocytes (Figure 5C). $CREB^{S111A}$ mice also exhibited elevated fasting glucose and increased body mass and adiposity under high fat diet feeding (Figure 5D–F) supporting the notion that phosphorylation of the ATM/CK cluster contributes to glucose metabolism and metabolic homeostasis *in vivo*.

DISCUSSION

The current model for CREB-mediated transcription invokes a two-hit mechanism in which the independent recruitment of CBP and CRTC coactivators is required for maximal CREB target gene induction (1). Our studies expand the CREB regulation paradigm to include autonomous, phosphorylation-dependent control of CREB DNA-binding activity. We propose that phospho-dependent regulation enhances the dynamic range of CREB-mediated transcription and speculate that such regulation may engender fine control at the level of individual CREB target genes and binding sites.

Previous experiments in the setting of DNA damage revealed that phosphorylation of the ATM/CK cluster diminished CBP/p300 binding (20), which is compatible with the location of the ATM/CK cluster near the KIX-interacting surface of the CREB KID. Although endogenously expressed $CREB^{S111A}$ exhibited elevated binding to the CBP KIX domain relative to WT CREB (Figure 2C), the finding that both CBP-dependent (AREG) and CBP-independent (CREM) genes underwent S111 phosphorylation-dependent attenuation following IR makes it unlikely that inhibition of CBP binding is the primary mechanism of CREB target gene attenuation. Instead, chromatin fractionation, DNA pull-down, ChIP and EMSA experiments point toward reductions in DNA binding activity and CRTC2 association as the major functional consequence of ATM/CK cluster phosphorylation. Regulation of CREB DNA binding activity through post-translational modification has been implied through a handful of studies (38–41). Most notably, Horiuchi and *et al*. demonstrated that phosphorylation of positionally conserved CK1/2 sites in *Drosophila* CREB inhibited its DNA-binding affinity *in vitro* (40). However, neither the regulatory mechanisms nor functional impacts of these phosphorylation sites were identified.

ATM/CK cluster phosphorylation inhibited CREB DNA binding and CRTC2 association in graded fashion proportionate to the number of phosphorylated residues. Under conditions of high DNA damage and maximal ATM activity, the ATM/CK cluster is stoichiometrically phosphorylated on all five sites and DNA binding at its minimum. Exposure to lower levels of DNA damage or cAMP (discussed below) leads to intermediate phosphorylation stoichiometries and intermediate DNA-binding affinities (Figure 5G). By preventing the phosphorylation of all five sites, the S111A mutation ostensibly abolished DNA damage-dependent attenuation of CREB DNA-binding activity, whereas S114A, S117A and S121A mutations—which have successively smaller impacts on ATM/CK cluster phosphorylation—had increasingly smaller impacts on DNA binding activity (Figure 5A). Although structural information is lacking, attenuation may involve allosteric communication between the intrinsically disordered KID and bZIP domain. Intrinsically disordered domains are increasingly recognized for their ability to form folded structures upon interaction with cognate binding partners, and these disorder to order transitions are often regulated through post-translational modification (42). Precedent for such a mechanism exists for Ets-1, where multisite phosphorylation of a Ser-rich region allosterically modulates the Ets-1 DNA-binding domain (43–45). An N-terminal fragment of CREB containing the ATM/CK cluster interacted with an extended CREB bZIP domain *in vitro*, though the phospho-dependence of this interaction could not be assessed (Figure 4D and E).

An unexpected finding from this study is that cAMP-induced phosphorylation of the ATM/CK cluster contributes to maximal CREB activation (Figure 1B). cAMP-induced phosphorylation of the ATM/CK cluster required PKA, but not S133 phosphorylation and was coupled to a functional DNA-binding domain (Figure 2B). Although the precise phosphorylation mechanism remains to be determined, it is plausible that DNA binding leads to a change in the ATM/CK cluster that renders it more accessible to CK1/2, and possibly, additional CREB kinases. That DNA binding strongly enhanced CREB phosphorylation lends credence to the idea that the KID and bZIP domains engage in bidirectional communication. How can cAMP-induced phosphorylation of the ATM/CK cluster promote transcriptional activation given its negative impacts on DNA binding? One parsimonious explanation for this paradox is that CREB proteins harboring a substoichiometric phosphorylation profile—and thus an intermediate affinity for DNA—are transcriptionally more potent than CREB proteins that are either unphosphorylated or fully phosphorylated. Whereas full phosphorylation of the ATM/CK clus-

←

90 min, irradiated with 20 Gy IR for 120 min (20 Gy) or treated with Fsk for 90 min after 20 Gy IR for 30 min (20 Gy-Fsk). *$P < 0.05$ (Student's *t*-test). (**D**) $CREB^{S111A}$ mice exhibit hyperglycemia. Fasting blood glucose levels were measured in 19-week-old male mice ($n = 7$ $CREB^{+/+}$ and 10 $CREB^{S111A}$, respectively) under fasted (16 h) conditions. (**E** and **F**) $CREB^{S111A}$ mice maintained on a high fat diet exhibit increased body weight (E) and adiposity (F). (**G**) Working model for phosphoregulation of CREB DNA binding activity in response to cAMP and DNA damage.

ter leads to overt chromatin eviction, intermediate CREB phosphorylation stoichiometries may reduce sequence nonspecific CREB DNA binding affinity, thereby increasing its sliding rate, and/or enable dynamic promoter exchange, which has been implicated in transcriptional activation by other TFs (46–48). Given CRTC2 recruitment defects in $CREB^{S111A}$ cells (Figure 3A), dynamic CREB-DNA interactions may also facilitate CRTC2 loading at CREB target gene promoters. Future studies will address whether the effects of ATM/CK cluster phosphorylation and CRTC2 loading can be genetically separated.

Physiologic importance of cAMP-induced ATM/CK cluster phosphorylation is supported by the blunted induction of gluconeogenic CREB target genes in $CREB^{S111A}$ livers and primary hepatocytes (Figure 5A–C). At the same time, $CREB^{S111A}$ mice exhibited elevated fasting glucose, suggesting that ATM/CK cluster phosphorylation is required for long-term glucose homeostasis. Conditional knockout of CREB in the liver did not lead to overt changes in gluconeogenesis or circulating glucose level (49), suggesting that glucose handling defects in $CREB^{S111A}$ mice occur through a dominant mechanism. Because $CREB^{S111A}$ was expressed in all tissues it is possible that hyperglycemia in $CREB^{S111A}$ mice is due to increased gluconeogenesis in the liver, defective pancreatic insulin secretion, global insulin resistance or a combination of mechanisms.

How CREB phosphorylation contributes to the ATM-dependent DNA damage response is presently unclear. Cell cycle checkpoint activation, proliferation rates, apoptosis and gross DBS repair were essentially normal in $CREB^{S111A}$ MEFs or hematopoietic tissues, suggesting that CREB phosphorylation does not make a major contribution to these established endpoints of ATM signaling. $CREB^{S111A}$ mice also did not exhibit elevated rates of tumorigenesis on the C57BL/6 background. Although we can only speculate, additional collaborating genetic insults may be required to unmask phenotypes associated with defective ATM-CREB signaling.

On the other hand, given that A-T patients and ATM knockout mice develop features of metabolic syndrome (23), it is conceivable CREB phosphorylation selectively plays a role in ATM-dependent metabolic regulation. Future studies using $ATM^{-/-}$ and $CREB^{S111A}$ mice will be needed to measure the activation and functional consequences of ATM-CREB signaling in liver under chronic conditions of HFD and other stress insults. Finally, it is worth considering that a role in transcriptional activation constitutes the primordial function of the ATM/CK cluster and that sequence differences between the ATM/CK clusters of mammalian CREB paralogs contribute to functional uniqueness. ATF1 is heavily phosphorylated on CK1/2 sites and undergoes additional phosphorylation by ATM in response to DNA damage, whereas CREM lacks ATM sites altogether (25). CK1/2 site are also present diverse metazoan CREB proteins from *Caenorhabditis elegans* to *Drosophila* whose regulation by DNA damage is uncertain. We speculate that cAMP-induced phosphorylation of CK1/2 sites evolved to enhance dynamic CREB–CRTC2–DNA interactions and transcriptional activation, whereas DNA damage-dependent regulation of this domain arose later during vertebrate evolution, potentially as an additional barrier to neoplastic growth.

SUPPLEMENTARY DATA

Supplementary Data are available at NAR Online.

ACKNOWLEDGEMENT

The authors wish to thank Qijing Xie for technical contributions and Dr Shigeki Miyamoto (UW-Madison Department of Oncology) and Dr Jerry Yin (UW-Madison Department of Genetics) for helpful discussions.

FUNDING

National Cancer Institute [R01CA180765-01 to R.S.T.]; National Institute for Neurological Disorders and Stroke [1R21NS090313-01A1 to R.S.T.]; National Institute of Diabetes and Digestive and Kidney diseases [R01DK090249 to C.R.J.]; Intramural Research Program of the National Institutes of Health [NIH]; National Institute of Environmental Health Sciences [NIEHS]. Funding for open access charge: National Cancer Institute [R01CA180765-01].
Conflict of interest statement. None declared.

REFERENCES

1. Altarejos,J.Y. and Montminy,M. (2011) CREB and the CRTC co-activators: sensors for hormonal and metabolic signals. *Nat. Rev. Mol. Cell Biol.*, **12**, 141–151.
2. Impey,S., McCorkle,S.R., Cha-Molstad,H., Dwyer,J.M., Yochum,G.S., Boss,J.M., McWeeney,S., Dunn,J.J., Mandel,G. and Goodman,R.H. (2004) Defining the CREB regulon: a genome-wide analysis of transcription factor regulatory regions. *Cell*, **119**, 1041–1054.
3. Zhang,X., Odom,D.T., Koo,S.-H., Conkright,M.D., Canettieri,G., Best,J., Chen,H., Jenner,R., Herbolsheimer,E., Jacobsen,E. *et al.* (2005) Genome-wide analysis of cAMP-response element binding protein occupancy, phosphorylation, and target gene activation in human tissues. *Proc. Natl. Acad. Sci. U.S.A.*, **102**, 4459–4464.
4. Oh,K.-J., Han,H.-S., Kim,M.-J. and Koo,S.-H. (2013) Transcriptional regulators of hepatic gluconeogenesis. *Arch. Pharm. Res.*, **36**, 189–200.
5. Kida,S. and Serita,T. (2014) Functional roles of CREB as a positive regulator in the formation and enhancement of memory. *Brain Res. Bull.*, **105**, 17–24.
6. Gonzalez,G.A. and Montminy,M.R. (1989) Cyclic AMP stimulates somatostatin gene transcription by phosphorylation of CREB at serine 133. *Cell*, **59**, 675–680.
7. Gonzalez,G.A., Yamamoto,K.K., Fischer,W.H., Karr,D., Menzel,P., Biggs,W., Vale,W.W. and Montminy,M.R. (1989) A cluster of phosphorylation sites on the cyclic AMP-regulated nuclear factor CREB predicted by its sequence. *Nature*, **337**, 749–752.
8. Yamamoto,K.K., Gonzalez,G.A., Biggs,W.H. and Montminy,M.R. (1988) Phosphorylation-induced binding and transcriptional efficacy of nuclear factor CREB. *Nature*, **334**, 494–498.
9. Mayr,B. and Montminy,M. (2001) Transcriptional regulation by the phosphorylation-dependent factor CREB. *Nat. Rev. Mol. Cell Biol.*, **2**, 599–609.
10. Radhakrishnan,I., Pérez-Alvarado,G.C., Parker,D., Dyson,H.J., Montminy,M.R. and Wright,P.E. (1997) Solution structure of the KIX domain of CBP bound to the transactivation domain of CREB: a model for activator:coactivator interactions. *Cell*, **91**, 741–752.
11. Chrivia,J.C., Kwok,R.P., Lamb,N., Hagiwara,M., Montminy,M.R. and Goodman,R.H. (1993) Phosphorylated CREB binds specifically to the nuclear protein CBP. *Nature*, **365**, 855–859.

12. Conkright,M.D., Canettieri,G., Screaton,R., Guzman,E., Miraglia,L., Hogenesch,J.B. and Montminy,M. (2003) TORCs: transducers of regulated CREB activity. *Mol. Cell*, **12**, 413–423.
13. Iourgenko,V., Zhang,W., Mickanin,C., Daly,I., Jiang,C., Hexham,J.M., Orth,A.P., Miraglia,L., Meltzer,J., Garza,D. *et al.* (2003) Identification of a family of cAMP response element-binding protein coactivators by genome-scale functional analysis in mammalian cells. *Proc. Natl. Acad. Sci. U.S.A.*, **100**, 12147–12152.
14. Bittinger,M.A., McWhinnie,E., Meltzer,J., Iourgenko,V., Latario,B., Liu,X., Chen,C.H., Song,C., Garza,D. and Labow,M. (2004) Activation of cAMP response element-mediated gene expression by regulated nuclear transport of TORC proteins. *Curr. Biol.*, **14**, 2156–2161.
15. Screaton,R.A., Conkright,M.D., Katoh,Y., Best,J.L., Canettieri,G., Jeffries,S., Guzman,E., Niessen,S., Yates,J.R., Takemori,H. *et al.* (2004) The CREB coactivator TORC2 functions as a calcium- and cAMP-sensitive coincidence detector. *Cell*, **119**, 61–74.
16. Luo,Q., Viste,K., Urday-Zaa,J.C., Senthil Kumar,G., Tsai,W.-W., Talai,A., Mayo,K.E., Montminy,M. and Radhakrishnan,I. (2012) Mechanism of CREB recognition and coactivation by the CREB-regulated transcriptional coactivator CRTC2. *Proc. Natl. Acad. Sci. U.S.A.*, **109**, 20865–20870.
17. Wang,J., Weaver,I.C.G., Gauthier-Fisher,A., Wang,H., He,L., Yeomans,J., Wondisford,F., Kaplan,D.R. and Miller,F.D. (2010) CBP histone acetyltransferase activity regulates embryonic neural differentiation in the normal and Rubinstein-Taybi syndrome brain. *Dev. Cell*, **18**, 114–125.
18. Ravnskjaer,K., Kester,H., Liu,Y., Zhang,X., Lee,D., Yates,J.R. and Montminy,M. (2007) Cooperative interactions between CBP and TORC2 confer selectivity to CREB target gene expression. *EMBO J.*, **26**, 2880–2889.
19. Xu,W., Kasper,L.H., Lerach,S., Jeevan,T. and Brindle,P.K. (2007) Individual CREB-target genes dictate usage of distinct cAMP-responsive coactivation mechanisms. *EMBO J.*, **26**, 2890–2903.
20. Shi,Y., Venkataraman,S.L., Dodson,G.E., Mabb,A.M., LeBlanc,S. and Tibbetts,R.S. (2004) Direct regulation of CREB transcriptional activity by ATM in response to genotoxic stress. *Proc. Natl. Acad. Sci. U.S.A.*, **101**, 5898–5903.
21. Shiloh,Y. and Ziv,Y. (2013) The ATM protein kinase: regulating the cellular response to genotoxic stress, and more. *Nat. Rev. Mol. Cell Biol.*, **14**, 197–210.
22. Valentin-Vega,Y.A., Maclean,K.H., Tait-Mulder,J., Milasta,S., Steeves,M., Dorsey,F.C., Cleveland,J.L., Green,D.R. and Kastan,M.B. (2012) Mitochondrial dysfunction in ataxia-telangiectasia. *Blood*, **119**, 1490–1500.
23. Schneider,J.G., Finck,B.N., Ren,J., Standley,K.N., Takagi,M., Maclean,K.H., Bernal-Mizrachi,C., Muslin,A.J., Kastan,M.B. and Semenkovich,C.F. (2006) ATM-dependent suppression of stress signaling reduces vascular disease in metabolic syndrome. *Cell Metab.*, **4**, 377–389.
24. Shanware,N.P., Trinh,A.T., Williams,L.M. and Tibbetts,R.S. (2007) Coregulated ataxia telangiectasia-mutated and casein kinase sites modulate cAMP-response element-binding protein-coactivator interactions in response to DNA damage. *J. Biol. Chem.*, **282**, 6283–6291.
25. Shanware,N.P., Zhan,L., Hutchinson,J.A., Kim,S.H., Williams,L.M. and Tibbetts,R.S. (2010) Conserved and distinct modes of CREB/ATF transcription factor regulation by PP2A/B56gamma and genotoxic stress. *PLoS One*, **5**, e12173.
26. Johnson,W.E., Li,C. and Rabinovic,A. (2007) Adjusting batch effects in microarray expression data using empirical Bayes methods. *Biostatistics*, **8**, 118–127.
27. Kerr,M.K., Martin,M. and Churchill,G.A. (2000) Analysis of variance for gene expression microarray data. *J. Comput. Biol.*, **7**, 819–837.
28. Kerr,M.K. and Churchill,G.A. (2001) Statistical design and the analysis of gene expression microarray data. *Genet. Res.*, **77**, 123–128.
29. Benjamini,Y. and Hochberg,Y. (1995) Controlling the false discovery rate: a practical and powerful approach to multiple testing on JSTOR. *J. R. Stat. Soc. B.*, **57**,289–300.
30. Kim,S.H., Shanware,N.P., Bowler,M.J. and Tibbetts,R.S. (2010) Amyotrophic lateral sclerosis-associated proteins TDP-43 and FUS/TLS function in a common biochemical complex to co-regulate HDAC6 mRNA. *J. Biol. Chem.*, **285**, 34097–34105.
31. Shi,Y., Dodson,G.E., Mukhopadhyay,P.S., Shanware,N.P., Trinh,A.T. and Tibbetts,R.S. (2007) Identification of carboxyl-terminal MCM3 phosphorylation sites using polyreactive phosphospecific antibodies. *J. Biol. Chem.*, **282**, 9236–9243.
32. Naqvi,S., Martin,K.J. and Arthur,J.S.C. (2014) CREB phosphorylation at Ser133 regulates transcription via distinct mechanisms downstream of cAMP and MAPK signalling. *Biochem. J.*, **458**, 469–479.
33. Kasper,L.H., Lerach,S., Wang,J., Wu,S., Jeevan,T. and Brindle,P.K. (2010) CBP/p300 double null cells reveal effect of coactivator level and diversity on CREB transactivation. *EMBO J.*, **29**, 3660–3672.
34. Walton,K.M., Rehfuss,R.P., Chrivia,J.C., Lochner,J.E. and Goodman,R.H. (1992) A dominant repressor of cyclic adenosine 3′, 5′-monophosphate (cAMP)-regulated enhancer-binding protein activity inhibits the cAMP-mediated induction of the somatostatin promoter in vivo. *Mol. Endocrinol.*, **6**, 647–655.
35. Nash,P., Tang,X., Orlicky,S., Chen,Q., Gertler,F.B., Mendenhall,M.D., Sicheri,F., Pawson,T. and Tyers,M. (2001) Multisite phosphorylation of a CDK inhibitor sets a threshold for the onset of DNA replication. *Nature*, **414**, 514–521.
36. Lee,C.W., Ferreon,J.C., Ferreon,A.C.M., Arai,M. and Wright,P.E. (2010) Graded enhancement of p53 binding to CREB-binding protein (CBP) by multisite phosphorylation. *Proc. Natl. Acad. Sci. U.S.A.*, **107**, 19290–19295.
37. Oh,K.-J., Han,H.-S., Kim,M.-J. and Koo,S.-H. (2013) CREB and FoxO1: two transcription factors for the regulation of hepatic gluconeogenesis. *BMB Rep.*, **46**, 567–574.
38. Grimes,C.A. and Jope,R.S. (2001) CREB DNA binding activity is inhibited by glycogen synthase kinase-3 beta and facilitated by lithium. *J. Neurochem.*, **78**, 1219–1232.
39. Bullock,B.P. and Habener,J.F. (1998) Phosphorylation of the cAMP response element binding protein CREB by cAMP-dependent protein kinase A and glycogen synthase kinase-3 alters DNA-binding affinity, conformation, and increases net charge. *Biochemistry*, **37**, 3795–3809.
40. Horiuchi,J., Jiang,W., Zhou,H., Wu,P. and Yin,J.C.P. (2004) Phosphorylation of conserved casein kinase sites regulates cAMP-response element-binding protein DNA binding in Drosophila. *J. Biol. Chem.*, **279**, 12117–12125.
41. Masson,N., John,J. and Lee,K.A. (1993) In vitro phosphorylation studies of a conserved region of the transcription factor ATF1. *Nucleic Acids Res.*, **21**, 4166–4173.
42. Wright,P.E. and Dyson,H.J. (2015) Intrinsically disordered proteins in cellular signalling and regulation. *Nat. Rev. Mol. Cell Biol.*, **16**, 18–29.
43. Desjardins,G., Meeker,C.A., Bhachech,N., Currie,S.L., Okon,M., Graves,B.J. and McIntosh,L.P. (2014) Synergy of aromatic residues and phosphoserines within the intrinsically disordered DNA-binding inhibitory elements of the Ets-1 transcription factor. *Proc. Natl. Acad. Sci. U.S.A.*, **111**, 11019–11024.
44. Pufall,M.A., Lee,G.M., Nelson,M.L., Kang,H.-S., Velyvis,A., Kay,L.E., McIntosh,L.P. and Graves,B.J. (2005) Variable control of Ets-1 DNA binding by multiple phosphates in an unstructured region. *Science*, **309**, 142–145.
45. Lee,G.M., Pufall,M.A., Meeker,C.A., Kang,H.-S., Graves,B.J. and McIntosh,L.P. (2008) The affinity of Ets-1 for DNA is modulated by phosphorylation through transient interactions of an unstructured region. *J. Mol. Biol.*, **382**, 1014–1030.
46. McNally,J.G., Müller,W.G., Walker,D., Wolford,R. and Hager,G.L. (2000) The glucocorticoid receptor: rapid exchange with regulatory sites in living cells. *Science*, **287**, 1262–1265.
47. Bosisio,D., Marazzi,I., Agresti,A., Shimizu,N., Bianchi,M.E. and Natoli,G. (2006) A hyper-dynamic equilibrium between promoter-bound and nucleoplasmic dimers controls NF-kappaB-dependent gene activity. *EMBO J.*, **25**, 798–810.
48. Shang,Y., Hu,X., DiRenzo,J., Lazar,M.A. and Brown,M. (2000) Cofactor dynamics and sufficiency in estrogen receptor-regulated transcription. *Cell*, **103**, 843–852.
49. Lee,D., Le Lay,J. and Kaestner,K.H. (2014) The transcription factor CREB has no non-redundant functions in hepatic glucose metabolism in mice. *Diabetologia*, **57**, 1242–1248.